3-1-2007

Induced Nested Galactic Bars Inside Assembling Dark Matter Halos

Clayton Heller
Georgia Southern University, cheller@georgiasouthern.edu

Isaac Shlosman
University of Kentucky, isaac.shlosman@uky.edu

Evangelie Athanassoula
Laboratoire d'astrophysique de Marseille, lia@lam.fr

Follow this and additional works at: https://digitalcommons.georgiasouthern.edu/physics-facpubs

Part of the Astrophysics and Astronomy Commons, and the Physics Commons

INDUCED NESTED GALACTIC BARS INSIDE ASSEMBLING DARK MATTER HALOS

CLAYTON H. HELLER,[1] ISAAC SHLOSMAN,[2] AND E. ATHANASSOULA[3]
accepted by the Astrophysical Journal Letters

ABSTRACT

We investigate the formation and evolution of nested bar systems in disk galaxies in a cosmological setting by following the development of an isolated dark matter (DM) and baryon density perturbation. The disks form within the assembling triaxial DM halos and the feedback from the stellar evolution is accounted for in terms of supernovae and OB stellar winds. Focusing on a representative model, we show the formation of an oval disk and of a first generation of nested bars with characteristic sub-kpc and a few kpc sizes. The system evolves through successive dynamical couplings and decouplings, forcing the gas inwards and settles in a state of resonant coupling. The inflow rate can support a broad range of activity within the central kpc, from quasar- to Seyfert-types, supplemented by a vigorous star formation as a by-product. The initial bar formation is triggered in response to the tidal torques from the triaxial DM halo, which acts as a finite perturbation. This *first* generation of bars does not survive for more than 4–5 Gyr: by that time the secondary bar has totally dissolved, while the primary one has very substantially weakened, reduced to a fat oval. This evolution is largely due to chaos introduced by the interaction of the multiple non-axisymmetric components.

Subject headings: galaxies: evolution – galaxies: formation – galaxies: halos – galaxies: kinematics and dynamics – galaxies: starburst – galaxies: structure

arXiv:astro-ph/0610428v3 26 Jun 2007

1. INTRODUCTION

The formation and evolution of galaxies are closely associated with the radial redistribution of baryonic and dark matter (DM) and of their angular momentum (J) (e.g., Athanassoula 2002, 2003). This process is further amplified by the lack of an axial symmetry in the basic galactic components over substantial periods of time. Numerical simulations have shown that DM halos form universally triaxial, i.e., flattened and elliptical[4] (e.g., Allgood et al. 2006), and remain in this state for the few Gyr during the disk growth (Berentzen & Shlosman 2006). A clear majority of disks are barred in the nearby universe (e.g., Knapen et al. 2000; Grosbol et al. 2004; Marinova & Jogee 2006), and a fraction of barred disks is maintained at least to $z \sim 1$ (Jogee et al. 2004; Elmegreen et al. 2004; Sheth et al. 2003). Simulations have also shown that galactic disks are subject to the spontaneous and induced stellar bar formation (e.g., Athanassoula 1984). A wide range of studies, theoretical and observational, argue that disk galaxies spend a substantial fraction of their life in a non-axisymmetric stage. Their morphological components are subjected to mutual gravitational torques that, in addition to external factors, provide an efficient mechanism for driving their internal evolution (e.g., Weinberg 1985; Athanassoula 1992; Heller & Shlosman 1994; Sellwood 2006).

The shapes of the host halos affect strongly the growing disk, especially because early disks are dominated by the *dissipative* baryonic component, unlike disks in the nearby universe. The gas responds dramatically to a non-axisymmetric driving by shocking and loses its rotational support. One can expect that bars or grand-design spiral arms will be triggered in the disk and that the central mass concentration will build up. The most efficient redistribution of J, down to the smallest radii, in a disk can be attributed to the mechanism of nested bars, stellar and gaseous, the so-called *bars-in-bars* scenario (Shlosman et al. 1989, 1990). The system of nested bars that consists of the primary (large-scale) and secondary (sub-kpc) bars tumbling with different pattern speeds, can facilitate the radial inflow of gas and fuel the accretion processes onto supermassive black holes (SBHs). The latter correlate tightly with the properties of galactic bulges across seven decades in radius at least (e.g., Ferrarese & Ford 2005). About 1/3 of barred galaxies have secondary bars (Laine et al. 2002; Erwin & Sparke 2002). Furthermore, formation of the SBH can be triggered by this process, because it leads to a specific entropy minimum in the center (Begelman et al. 2006). The dynamics of nested bars has been investigated (e.g., Shlosman et al. 1989; Friedli & Martinet 1993; Combes 1994; Maciejewski & Sparke 2000; Heller et al. 2001; Shlosman & Heller 2002; El-Zant & Shlosman 2003), but modeling of nested bars in a cosmological scenario even for isolated DM halos was never attempted or validated.

This Letter demonstrates how a nested bar system forms in a disk growing in an assembling triaxial DM halo. We use cosmological initial conditions and follow the Hubble expansion and the subsequent collapse of an isolated perturbation in the gas and the DM. Our star formation (SF) algorithm is physically motivated and we include feedback from stellar evolution. A large number of models have been run and show the formation of galactic disks whose structural parameters fit within the observed range. Here we describe a representative model only and focus on the formation of nested bars. Additional aspects will be addressed elsewhere.

[1] Department of Physics & Astronomy, Georgia Southern University, Statesboro, GA 30460, USA
[2] Department of Physics and Astronomy, University of Kentucky, Lexington, KY 40506-0055, USA
[3] Observatorie de Marseille, 2 Place Le Verrier, 13248 Marseille Cedex 04, France
[4] We define the density (equatorial) ellipticity as $\epsilon_\rho = 1 - b/a$ — where b/a is the intermediate-to-major axis ratio and the flatness as $f_\rho = 1 - c/a$, where c/a — the minor-to-major axis ratio

2. NUMERICS, STAR FORMATION, FEEDBACK AND INITIAL CONDITIONS

The simulations were performed with an updated version of the FTM-4.4 hybrid N-body/SPH code (Heller & Shlosman 1994), using the routine `falcON` (Dehnen 2002) to compute the forces. The gas temperature was obtained from the energy equation. We used $N_{\rm DM} = 5 \times 10^5$ and $N_{\rm SPH} = 5 \times 10^4$, gravitational softening of 150 pc for DM and stars, and dynamic softening with a minimum of 250 pc for the gas. Tests have been performed to check the sensitivity of the results to the algorithm and its parameters. A pure DM run conserved the energy to within 1% and J to within 0.1%.

The modified prescription for SF and the feedback from stellar evolution take place in the Jeans unstable, contracting region. We fix the gas-to-background density at which gas is converted to a star, the local collapse-to-free fall time, and introduce the probability that the gas particle produces a star during a given timestep. Four generations of stars form per gas particle with an instantaneous recycling along with an increment in metallicity. The balance of the specific internal energy along with the gas ionization fractions of H and He and the mean molecular weight are computed as a function of ρ and T for an optically thin primordial composition gas. Feedback from stellar evolution includes the supernovae and OB stellar winds, and uses the thermalization parameter — a fraction of the feedback deposited as a thermal energy, and converted into kinetic energy via equations of motion (Heller et al., in prep.).

The initial conditions are those of a spherically-symmetric density enhancement at $z = 36$ evolved using an open CDM (OCDM) model with $\Omega_0 = 0.3$, $h = 0.7$. The difference between the OCDM and ΛCDM is minimal on sub-galactic scales. The initial density profile corresponds to the average density around a 2σ peak in a Gaussian random density field. The spin parameter $\lambda = 0.05$ is set by the angular velocity $\omega \propto r^{-1}$, where r is the cylindrical radius and the central kpc has been softened. We impose the collapse redshift of $z = 2$. The mass of collisionless DM particles is 7×10^{11} M$_\odot$ and the gas comprises 10% of the total mass initially.

The main simplification in our models is that we neglect interactions and minor or major mergers. Yet, because the evolution is determined to a large extent by the nonlinear interaction between three non-axisymmetric components, the results presented here can be considered representative.

3. RESULTS

The initial perturbation expands with the Hubble flow and collapses, forming a DM halo — a nearly *nonrotating* triaxial figure. In particular, the innermost 10 kpc experience a very abrupt and short-lived increase of their ellipticity to ϵ_ρ 0.2, presumably due to radial orbit instability. The disk grows within the halo equatorial plane, visible already at $\tau \sim 0.5$ Gyr. Its growth nearly washes out the inner, < 10 kpc, halo ellipticity, due to the increased central mass concentration in the system and the out-of-phase response by the disk. The inner 5 kpc (10 kpc) of the DM become nearly axisymmetric and only slightly flattened after ~ 2 Gyr (~ 7 Gyr), while at larger radii $\epsilon_\rho \to 0.15 - 0.25$ and $f_\rho \to 0.3 - 0.4$.
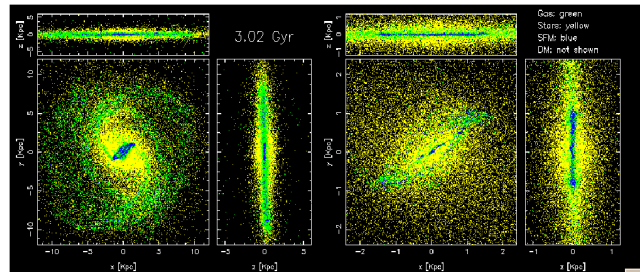
The disk evolution consists of gas-dominated (first

$1.5 - 2$ Gyr) and star-dominated phases (Fig. 1 and Animation Seq. 1). The ratio of baryonic-to-DM matter within the central 10 kpc increases from ~ 0.4 to ~ 0.54 over the Hubble time due to an adiabatic contraction. The corresponding pure DM model results in the NFW (Navarro et al. 1996) density profile and the characteristic radius $R_{\rm nfw} \sim 9$ kpc and is even more triaxial. For the model with baryons — $R_{\rm nfw} \sim 4.5$ kpc, and the fit quality has worsened. The cusp is baryon-dominated.

Initially, the disk is roughly oval and dominated in the outer parts by $m = 2$ and 3 grand-design spirals. Gradually it becomes more axisymmetric. The characteristic time for the disk (and halo) buildup, i.e., reaching 50% of its mass at $z = 0$, is ~ 1.5 Gyr. The rate of a baryonic inflow into the disk region crests within 1 Gyr. The SF rate shows a similar behavior.

The disk grows from inside out. A primary ~ 2 kpc-radius bar appears in the stellar component around 0.6 Gyr *normal* to the halo major axis, increasing to 3 kpc by 0.7 Gyr. By 0.8 Gyr, the inner part of the 4 kpc bar, which is gas-dominated, decouples in the prograde direction and forms a secondary bar. By 1.5 Gyr, most of the gas in the secondary has fallen to the center — further collapse is inhibited by the numerical resolution.

Fig. 2a follows the evolution after 1 Gyr. Both bars are strong at this time, as given by $A_2 \sim 0.6$ and 0.45 — the amplitudes of corresponding $m = 2$ modes. They are SF-dominated and involve a large fraction of the stellar and gas disk mass. The shape of the primary depends strongly on its orientation with respect to the halo *and* disk major axes — main sources of tidal torques — and on its internal (self-gravitational) response, e.g., between 1 to 2 Gyr (Anim. Seq.). The disk response to the halo torques drives a pair of strong grand-design arms whose pitch angle gradually decreases forming a pseudo-ring outside the bar, after which the open arms are regenerated (Anim. Seq.). The bars appear to decay after ~ 1.7 Gyr in tandem with the arms, but strengthen abruptly after 2 Gyr. The primary weakens again after 2.5 Gyr, while the secondary bar dissolves by ~ 5 Gyr. The bar sizes vary between $r_{\rm s} \sim 0.5 - 1$ kpc for the secondary and $r_{\rm p} \sim 5 - 7$ kpc for primary bars.

The central issue of bars-in-bars systems is the *dynamical coupling* of bars as measured by the ratio of pattern
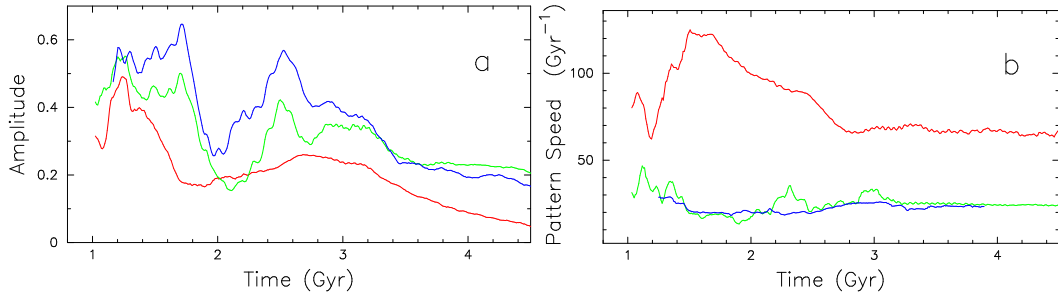
FIG. 2.— Nested bars evolution: (a) $m = 2$ amplitudes A_2, and (b) associated pattern speeds. Shown are the stellar A_2 and pattern speeds of the secondary (red line) and primary (green line) bars and of the oval disk, between $5 - 10$ kpc (blue line).
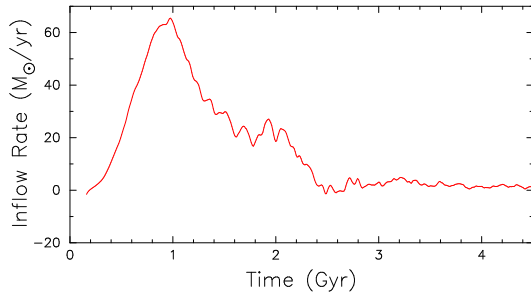

FIG. 3.— Gas inflow rate across the central kpc.

speeds, Ω_s/Ω_p (Fig. 2b). The primary bar slows down prior to 1.5 Gyr, tumbles with a constant Ω_p over the next 1 Gyr, speeds up and stabilizes around 2.8 Gyr for the rest of the simulation time. The secondary bar speeds up dramatically before 1.5 Gyr, stabilizes for ~ 0.2 Gyr, then slows down and stabilizes again after 2.8 Gyr. Its Ω_s appears to have a plateau also around 2.4 Gyr. Hence the bars go over a number of stages with various $\Omega_s/\Omega_p \approx const$.

Additional evidence for coupled evolution comes from varying corotation (CR) radii, $r_{cr,s}$ and $r_{cr,p}$, of bars and from the position of the inner Lindblad resonance (ILR) of the primary, $r_{ILR,p}$. During the first 1.5 Gyr, $r_{cr,s}$ and $r_{cr,p}$ increase sharply from ~ 1 kpc and 4.2 kpc to 2.3 kpc and 8.2 kpc, respectively. This increase is caused by a substantial inflow that leads to a surge of the rotation curve. This is followed, between $1.5 - 2.8$ Gyr, by a plateau in $r_{cr,s}(\tau)$ and $r_{cr,p}(\tau)$, and a further increase of $r_{cr,s}$ to 3.5 kpc. Both remain stable thereafter. We estimate $r_{cr,p}/r_p \sim 1.1 - 1.6$ and $r_{cr,s}/r_s \sim 1.3 - 5$. The value of 5 is achieved at the end of the first 1.5 Gyr (it results from the runaway action of the gas-dominated secondary, see §4), and after 2.8 Gyr — making the secondary much shorter than its CR. The ILR of the primary can be inferred to lie outside the nuclear ring (see below) during this stage, $r_{ILR,p} \sim 3.5$ kpc.

Nuclear rings form at the interface between the bars, and a pair of grand-design arms extend along the primary — the ring and the arms are delineated by the SF intermittently. The ring evolution is more dramatic when viewed in the SF colors and it fades away with the weakening of the primary.

4. DISCUSSION

We have simulated, in a large number of models, the formation of galactic disks in assembling triaxial DM halos and analyzed a representative model. The accompanying SF and the stellar feedback have been included. We followed the collapse of an isolated cosmological density perturbation with $\lambda = 0.05$ from its linear regime, in the OCDM universe. The disk and halo form, i.e., reach 50% of their final mass, over a period of ~ 1.5 Gyr. The DM halo develops a clear triaxial shape, elliptical in the plane perpendicular to the original angular momentum axis and flattened along this axis. The resulting halo figure tumbles very slowly, $\sim \pi$ over the Hubble time.

The halo triaxiality decreases during the disk growth because of the increasing central mass concentration and the disk response to the halo potential. The first effect reduces somewhat f_ρ and ϵ_ρ of the halo, even in the absence of a baryonic component. The second effect results from the negligible tumbling of the halo figure — the inner ILR and the outer ILR are pushed to the center and to large radii, respectively. The disk responds out-of-phase with the halo potential, thus diluting the halo ellipticity in its equatorial plane. This effect is not related to dissipation.

Most importantly, the halo torques lead to a strongly oval-shaped, growing disk and trigger the bar formation — reminiscent of torques exerted on the disk during galaxy interactions. *These initial bars form as a result of a finite amplitude perturbation and not as a consequence of an exponential growth from an infinitesimal perturbation.* Their formation timescale is much shorter than for spontaneous bars and they appear first normal to the halo major axis. In our simulation the initial triaxiality of the inner halo is due to a short-lived episode of the radial orbit instability erasing the initial conditions (e.g., MacMillan et al. 2006). Other causes of triaxiality are possible — we wish to stress here its effect on bar formation and evolution.

While nested bars have been simulated before, with various degrees of self-consistency, this simulation differs in at least four major aspects. First, this is the most self-consistent model of nested bars in the literature — no *a priori* assumptions have been made. Second, this is the first model where nested bars form from cosmological initial conditions. Third, both bars are very gas rich, while previous models of nested bars focused on purely stellar or gaseous bars (Shlosman 2005, for review). Fourth, we have incorporated SF and feedback —

the stellar and gaseous masses in the simulations are not individually conserved.

It is helpful to divide the nested bar evolution into three distinct phases, namely formation, dynamical adjustment and dynamically quiescent phases, as exhibited in Fig. 2b. The *initial phase*, which is preceded by an early disk, ends at ~ 1.5 Gyr and extends over ~ 0.7 Gyr from the time the secondary can be identified. The primary and especially secondary bars form gas rich. During this time, Ω_p decays steadily while Ω_s increases monotonically by a factor of ~ 2. The latter increase is due to the gas collapse by a factor of 3–4 within the secondary, down to numerical resolution scales. Simulations of a dynamical runaway of a pure gaseous secondary have shown $\Omega_s \sim r_s^{-1}$ (Englmaier & Shlosman 2004). A smaller growth in Ω_s in our model can be explained if a correction is made for the non-dissipative stellar component in the bar. Note that Ω_p follows closely the pattern speed of the oval disk, which forms in response to the halo ellipticity (Fig. 2b).

The *second phase* of evolution, between 1.5 – 2.8 Gyr, is characterized by a dynamical adjustment of primary and secondary bars via their pattern speeds. The ratio $\Omega_s/\Omega_p \sim 6.1$ is steady for about 0.2 Gyr, then decays steadily because of a monotonic decrease in Ω_s, while Ω_p stays constant initially, then increases slowly. The bars pass through an intermediate period of ~ 0.2 Gyr when their pattern speeds are possibly locked, $\Omega_s/\Omega_p \sim 4.4$, at about 2.4 Gyr. A dramatic inflow leads to a buildup of a massive gas disk that generates grand-design shocks in response to the (elliptical) halo driving when the disk ellipticity surpasses a critical value (B. Pichardo & I. Shlosman, 2005, unpublished). This process largely determines Ω_p which is also the pattern speed of the spiral arms. Hence, contrary to other models, the overall evolution in the system is driven by the halo triaxiality.

While the disk shape depends strongly on the angle with the halo major axis, the primary bar is shaped by the angle with the halo *and* with the oval disk — an efficient way to amplify chaos within the bar, weakening it on a short timescale (El-Zant & Shlosman 2002; Berentzen et al. 2006; Berentzen & Shlosman 2006). This can explain the sharp decay of primary amplitude

at 1.7 Gyr and 2.5 Gyr, both accompanied by massive spiral arms in the disk. Secondary bars have been found to adjust their properties, such as axial ratios and radial extent, depending on the mutual bar orientation (Heller et al. 2001; Shlosman & Heller 2002). The situation is much more complex in the present run, because a number of *a*symmetric components coexist. The individual interactions, which are not always possible to disentangle, will increase the fraction of chaotic orbits in the bars and generate local (non-grand-design) shocks in the gas. These interdependencies can have observational corollaries at redshifts corresponding to disk growth and will be addressed elsewhere.

The *third phase,* after ~ 2.8 Gyr when the gas fraction is low, is that of a stable coupling between Ω_p and Ω_s, i.e., $\Omega_s/\Omega_p \sim 2.7$, confirming that *stellar* nested bars can be long-lived systems (El-Zant & Shlosman 2003). Because $r_{ILR,p} \sim r_{CR,s}$ at this time (see §3), it is possible that we observe a resonant coupling between primary and secondary as proposed by Tagger et al. (1987) for any two modes.

During the first stage, the gas inflow across the central kpc, $\dot{M}_1$, corresponds to a quasar-type activity of 60 M$_\odot$ yr^{-1} (Fig. 3), while the SF peaks at 25 M$_\odot$ yr^{-1}. In the second stage, $\dot{M}_1$ crests at ~ 25 M$_\odot$ yr^{-1} around 2 Gyr, dropping to its lowest value close to zero thereafter. Nuclear rings and the associated SF are intimately related to this inflow (Athanassoula 1992; Heller & Shlosman 1996; Knapen 2005), but in nested bars they vary in shape and have a more limited life span in response to the time-dependent potential (Shlosman & Heller 2002).

Hence, we have demonstrated that nested bars in isolated halos form from cosmological initial conditions and go through a series of dynamical couplings and decouplings, while channeling the gas inwards to the smallest scales resolved numerically. This inflow can support the early quasar-type and Seyfert-type activity thereafter. The exact conditions leading to an SBH formation (Begelman et al. 2006) are beyond the scope of this work, but the remote 'boundary' conditions are in agreement.

REFERENCES

Allgood, B., Flores, R.A., Primack, J.R., Kravtsov, A.V., Wechsler, R.H., Faltenbacher, A., Bullock, J.S., 2006, MNRAS, 367, 1781
Athanassoula, E. 1984, Phys. Reports, 114, 320
Athanassoula, E. 1992, MNRAS, 259, 345
Athanassoula, E. 2002, ApJ, 569, L83
Athanassoula, E. 2003, MNRAS, 341, 1179
Begelman, M.C., Volonteri, M., Rees, M.J. 2006, MNRAS, 370, 289
Berentzen, I. Shlosman, I., Jogee, S. 2006, ApJ, 637, 582
Berentzen, I. Shlosman, I. 2006, ApJ, 648, 807
Combes, F. 1994, in Mass-Transfer Induced Activity in Galaxies, (ed.) I.Shlosman, CUP, 170
Dehnen, W. 2002, J. Comp. Phys., 179, 27
Elmegreen, B.G., et al. 2004, ApJ, 612, 191
El-Zant, A., Shlosman, I. 2002, ApJ, 577, 626
El-Zant, A., Shlosman, I. 2003, ApJ, 595, L41
Englmaier, P., Shlosman, I. 2004, ApJ, 617, L115
Erwin, P., Sparke, L.S. 2002, AJ, 124, 65
Ferrarese, L., Ford, H. 2005, Space Sci. Rev., 116, 523
Friedli, D., Martinet, L. 1993, A&A, 277, 27
Grosbol, P., Patsis, P.A., Pompei, E. 2004, A&A, 423, 849
Heller, C.H., Shlosman, I. 1994, ApJ, 424, 84
Heller, C.H., Shlosman, I. 1996, ApJ, 471, 143
Heller, C.H., Shlosman, I., Englmaier, P. 2001, ApJ, 553, 661

Jogee, S., Barazza, F.D., Rix, H.-W., Shlosman, I., et al. 2004, ApJ, 615, L105
Knapen, J.H., Shlosman, I., Peletier, R.F. 2000, ApJ, 529, 93
Knapen, J.H. 2005, A&A, 429, 141
Laine, S., Shlosman, I., Knapen, J.H., Peletier, R.F. 2002, ApJ, 567, 97
Maciejewski, W., Sparke, L.S. 2000, MNRAS, 313, 745
MacMillan, J.D., Widrow, L.M., Henriksen, R.N. 2006, astro-ph/0604418
Marinova, I., Jogee, S. 2006, astro-ph/0608039
Navarro, J.F., Frenk, C.S., White, S.D.M. 1996, ApJ, 462, 563 (NFW)
Sellwood, J.A. 2006, ApJ, 637, 567
Sheth, K., Regan, M.W., Scoville, N.Z., Strubbe, L.E. 2003, ApJ, 592, L13
Shlosman, I., Frank, J., Begelman, M.C., 1989, Nature, 338, 45
Shlosman, I., Begelman, M.C., Frank, J. 1990, Nature, 345, 679
Shlosman, I., Heller, C.H. 2002, ApJ, 565, 921
Shlosman, I. 2005, in The Evolution of Starbursts, S. Huettemeister & E. Manthey (eds.), Melville: AIP, p. 223
Tagger, M., Sygnet, J.F., Athanassoula, E., Pellat, R. 1987, ApJ, 318, L43
Weinberg, M. D. 1985, MNRAS, 213, 451